Capacitor volume evaluation based on ripple current in Modular Multilevel Converter

Toshiki Nakanishi[1], and Jun-ichi Itoh[1]

[1] Nagaoka University of Technology, 1603-1 Kamitomioka, Nagaoka, Niigata, Japan

Abstract-- **This paper discusses the overall volume evaluation of capacitors in Modular Multilevel Converter (MMC). First, a theoretical formula of the ripple voltage on each cell capacitor in the MMC is clarified. Second, a formula of the total electrostatic energy is clarified. As a result, it is difficult to evaluate the overall volume of the capacitors because the total electrostatic energy is constant even the number of cells changes. Against the problem, the overall volume of the capacitors is designed by using the database of commonly-marketed electrolytic capacitors which are generally implemented into many products. In conclusion, the parallel connection of the capacitor with the small ripple current is better than using one capacitor with the large ripple current in order to achieve the size reduction of capacitors. Finally, it is necessary to close the ratio of the charge voltage to the withstand voltage to 1.0 in order to achieve the volume minimization.**

Index Terms—**Modular Multilevel Converter, Step-down rectifier, DC micro-grid, Capacitor volume evaluation.**

I. INTRODUCTION

Recently, a micro-grid and a DC power grid have been actively researched as next generation power supplies [1]-[3]. Specifically, the DC micro-grid is suitable to connect a battery energy storage system and a renewable energy source such as a photovoltaic generation system or a fuel cell to the DC grid because the output voltages of many renewable energy sources are DC voltage [1]-[3]. From the above advantages, the micro-grid has been applied to the power grid in isolated islands as a stand-alone power system [3]. Moreover, an offshore wind power generation system is also actively researched [3]. The wind power generation is able to apply as the power source in isolated islands because weather conditions around isolated islands are suitable for the wind power generation.

Presently, the wind power generation system which is connected to an AC grid has a transformer between the generator and the power converter in order to match the generator voltage and the AC grid voltage [4]. In the case of the wind power generation system which is connected to the DC micro-grid, the step-down rectification is required because the voltage rating of the wind power generator with high power capacity is higher than the DC bus voltage in the DC micro-grid. Specifically, the voltage rating of the wind power generator is several kilovolts [5]. On the other hand, the DC bus voltage in the DC micro-grid is 400 V [2]. The step-down operation is able to be achieved simply by the transformer. However, the volume of the transformer is bulky. The main reason why the transformer becomes bulky is that the operation frequency of the transformer is low, because the transformer is required to operate in synchronization with the low generator frequency. Moreover, the reasons why the transformer is bulky includes that the high transform ratio is required.

As one of solutions, the employment of Modular Multilevel Converter (MMC) to the wind power generation system connected to the micro-grid is an effective method. The MMC has been actively researched as a next generation high power converter without the bulky transformer [6]-[7]. Therefore, the wind power generation system achieves the size reduction by applying the MMC into the system. However, in the general AC-DC converter using the MMC which consists of chopper cells, it is difficult to achieve the step-down rectification because chopper cells cannot output the negative voltage.

In order to overcome the above problem, a step-down converter using the MMC with H-bridge cells has been proposed [6]-[7]. The MMC with the H-bridge cells achieves the reduction of the bulky transformer because the H-bridge cell has no limit of the output voltage. Thus, the system with the H-bridge cells operates as a high power step-down rectifier. On the other hand, the design method of the capacitance in each cell and the overall volume evaluation when the number of cells is changed, have been reported scarcely [8]. So far, the volume of the capacitor based on the electrostatic energy has been reported [8]. However, it is seems that the relationship between the capacitor volume and the number of cells has not been reported. Specifically, it is important to consider a ripple current of the capacitors in terms of lifetime of the capacitor when the capacitor with the large capacity such as an electrolytic capacitor is applied.

This paper discusses the overall volume evaluation of the capacitors in the MMC. First, a formula of the total

electrostatic energy is clarified by using a formula of the capacitance, because the capacitance is designed in order to suppress the ripple voltage. As a result, the electrostatic energy does not change even the number of cells changes because the formula of the total electrostatic energy does not include the number of cells as a variable number. Thus, it is necessary to evaluate the volume of the capacitors by other methods. On the other hand, the volume of the capacitors changes when the capacitor parameters such as the voltage rating and the capacitance changes. Moreover, the ripple current of the capacitor is one of the important factors for the capacitor design when the electrolytic capacitors are applied. Therefore, it is necessary to evaluate the relationship between the ripple current and the volume of the capacitors as a first step of the capacitor design. In this paper, the overall volume of the capacitors is evaluated by applying the database of commonly-marketed electrolytic capacitors which are generally implemented into many products. Finally, the relationship between the overall volume and the number of cells is shown.

II. Step-down Rectifier using MMC for Wind Power Generation System connected to DC Micro-grid

A. Main circuit configuration

Fig. 1 shows the main circuit configuration of the proposed step-down rectifier using the MMC. Each leg consists of two buffer reactors L_b and the H-bridge cells. The converter outputs a multi-level voltage waveform in order to reduce harmonic distortions of the input current. Thus, many cascaded cells are used in practical because the reduction effect of the harmonic distortion increases by increasing the number of cells. Additionally, the MMC is able to reduce the voltage rating of devices on each cell because of cascade connections of cells. Therefore, lower voltage rating devices are utilized to the MMC. On the other hand, the output DC voltage of the MMC depends on the sum of the cell's output average voltage. Thus, the output voltage of the cell includes the AC component and the DC component in order to control the input current and the output voltage. Moreover, the MMC converts the high AC voltage to the DC voltage of several hundreds volts. After this step, the DC voltage of 400 V is supplied to the DC bus of the DC distribution by an isolated DC-DC converter. Thus, the input side and the output side are isolated by the DC-DC converter.

B. Relationship between cell configurations and output voltage

Fig. 2 shows relationships between cell configurations and cell output voltages. In the AC-DC converter using the MMC, the maximum value of the generator output voltage is applied to each arm of the MMC when the wind generator operates. Thus, the peak-to-peak value of the cell output voltage $v_{p\text{-}p}$ is given by (1) from the generator output voltage and the number of cells per leg.

$$v_{p-p} = 4\sqrt{\frac{2}{3}}\frac{E}{n} \tag{1}$$

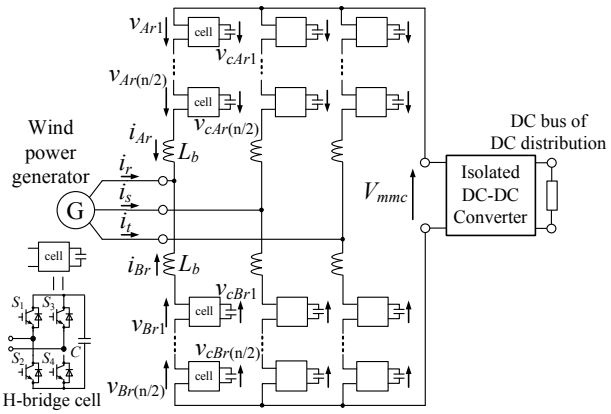

Fig. 1. Circuit configuration of the MMC for the wind power generation system connected to the DC micro-grid. The MMC with the H-bridge cells is able to operate as the step-down rectifier.

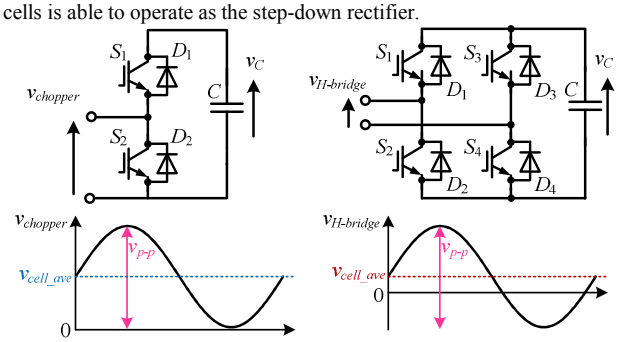

(a) Chopper cell (b) H-bridge cell

Fig. 2. Circuit configuration and output voltage of each cell. The chopper cell has the lower limit of the output voltage because the chopper cell cannot output the negative voltage. On the other hand, the H-bridge cell does not have the lower limit of the output voltage.

where E is an effective value of an output line-to-line voltage in the wind power generator, and n is the number of cells at each leg.

In addition, the output DC voltage of the AC-DC converter using the MMC V_{mmc} equals to the sum of the cell's average output voltage at one leg. Hence, V_{mmc} is given by (2).

$$V_{mmc} = nv_{cell\_ave} \tag{2}$$

where v_{cell_ave} is an average output voltage of one cell.

Fig. 2(a) shows the relationship between the chopper cell and its output voltage. In the case of applying the chopper cell, the lower limit of the cell's output average voltage is uniquely determined from the peak-to-peak value of the cell voltage $v_{p\text{-}p}$ and the number of cells at each leg n, because the chopper cell cannot output the negative voltage. Therefore, in the chopper cell, the lower limit of the cell's output average voltage is given by (3).

$$v_{cell\_ave} = \frac{1}{2}v_{p-p} \tag{3}$$

From (1), (2) and (3), the lower limit of the output DC voltage V_{mmc} equals twice the value of a maximum voltage of the wind generator phase voltage. From the above principle, the MMC with chopper cells cannot achieve the step-down rectification.

Fig. 2(b) shows the relationship between the H-bridge cell and its output voltage. In the case of the H-bridge cell, there is no limit of cell output average voltage because it

is possible for the H-bridge cell to output the negative voltage. Hence, the H-bridge cell is able to control lower voltage than that of (3). Therefore, the MMC with the H-bridge cells achieves the step-down rectification.

III. Control Strategy

Fig. 3 shows the control block diagram of the proposed step-down converter. The proposed control system is based on the single-phase power factor correction (PFC) converter because the H-bridge cell has same circuit configuration as singe-phase PFC converter. Moreover, the PFC converter and the H-bridge cell have many common points in the circuit operation and the control system. For example, the capacitor voltage has to be maintained constant in both circuits. Moreover, each converter has to control the input AC current in order to maintain the capacitor voltage and reduce the total harmonic distortion (THD). Differences between the PFC converters and the H-bridge cells are; there is the DC component in the output voltage of the H-bridge cell, and a voltage balancing control is necessary in order to correct unbalance voltages among all capacitors. Thus, in order to deal with above problems, it is necessary to add two control systems to control the DC component and achieve the voltage balancing into the conventional control system of the PFC converters.

Specifically, in order to control each arm as shown in Fig. 1, the control block diagram is separated to the capacitor voltage control block and the input current control (ACR) block. Moreover, the capacitor voltage control block consists of an average voltage control (AVR) system and a voltage balancing control system. First, the average voltage control system regulates the average value of the capacitor voltage in the arm into the capacitor voltage command. On the other hand, the voltage balancing control system corrects the unbalance among all capacitor voltages in the arm.

Moreover, the PI controller in AVR outputs the positive phase component's command of the arm current. Therefore, the positive phase component of the arm current is regulated in order to keep the capacitor voltage constant. On the other hand, the zero phase component of the arm current is controlled in order to supply the output power to the DC micro-grid side.

A. Average Voltage Control

The average voltage control is applied in order to control the average value of all capacitor voltage in the arm [6]. Therefore, the average value of all capacitor voltages has to be calculated in each arm.

The error between the capacitor voltage command and the average value of all capacitor voltages in the arm is corrected by a PI controller. The output value of the PI controller is given as the positive phase component's command of the arm current.

Moreover, the H-bridge cell outputs the DC voltage in order to achieve the rectification. Therefore, the capacitor voltage includes the ripple voltage whose cycle is same as the input AC voltage. It should be cautious the control system may become instability due to the ripple voltage.

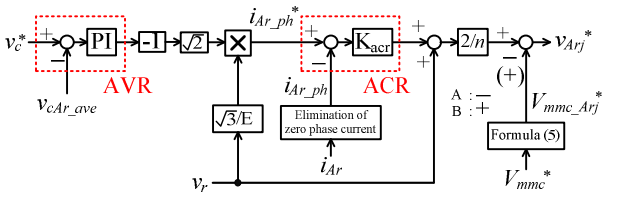

Fig. 3. Control block diagram for step-down rectifier using the MMC. The proposed control is based on a control system of a single-phase power factor correction (PFC) converter. The proposed control system is applied to each arm of the MMC in order to control each arm. Moreover, the ACR controls only the AC component of the arm current.

Thus, in order to keep the stability of the control system, a filter in order to damp the frequency component of the input voltage cycle should be applied.

B. Arm Current Control

Each arm current includes the AC component and the DC component. First, the AC component of the arm current flows from the wind power generator. The AC component is defined as the positive phase component. Moreover, from the previous section, the positive phase component's command is generated by the average voltage control. In other words, the AC component of the arm current is controlled in order to maintain the average value of all capacitor voltages in each arm constant.

The PFC operation in the input side of the MMC is achieved in the control system by regulating only the AC component of the arm current. Furthermore, as the generator control system, it is necessary for the proposed control system to achieve the high efficiency at same time. In general, the $i_d = 0$ control is applied in order to achieve the high efficiency in a lot of adjustable drive systems. In the proposed converter, the control system achieves the $i_d = 0$ control by conforming the phase of the positive phase current's command to the back electromotive force (back-EMF)'s one of the wind power generator.

On the other hand, the DC component of the arm current flows in order to supply the DC power into the load. The DC current shunts into the each leg of the MMC. Generally, the shunted DC current is constant and has same value among arms when the output DC voltage of the MMC is divided equally among cells. The DC current is considered as the zero phase component because the DC current is constant at a specific load.

In the ACR, it is necessary to eliminate only the zero phase component from the arm current in order to control the capacitor voltage. However, it is difficult for a high-pass filter to extract only the positive phase component because the AC current frequency is very low. The methods to extract the positive phase component have been proposed [6]. In this paper, the application of the rotational coordinate transform is applied. This method extracts the positive phase component by using the rotational coordinate transform in each arm group; the upper side and the lower side. The zero phase component is eliminated by the rotational coordinate transform and the inverse transform.

C. Output Voltage Control System

The output DC power is controlled by the zero phase component. The command of the output DC voltage is

added into the output value of the controller in the arm current control system. Moreover, the output DC voltage of the MMC is divided on each leg. Thus, the output DC voltage of one cell is fundamentally set as V_{mmc}^{*}/n when the command of the MMC output voltage control is V_{mmc}^{*}.

D. Voltage Balancing Control System

The average voltage control is used to maintain the average value of all capacitor voltage. However, an unbalance voltage which occurs among capacitors in same arm cannot be suppressed by only the average voltage control, because the average voltage control corrects only the error between the voltage command and the average value of all capacitor voltages in the arm. So far, several methods to balance each capacitor voltage have been reported [7], [9]. However, in most of the conventional control systems, it is difficult to understand these control principle. Moreover, a design method of control parameters has not been reported. In the control method of this paper, the positive phase component of the arm current is applied in order to maintain the average value of all capacitor voltages in each arm. Therefore, the common positive phase component flows into all cells in same arm. Thus, it is difficult to adjust the positive phase component of the arm current in order to balance the capacitor voltage on each cell. In order to solve this problem, in the proposed control system, the output DC voltage of the cell is varied depending on the capacitor voltage. The control principle is given by (4).

$$V_{mmc\_mkj}^{*} = A_{vd\_mkj} V_{mmc}^{*} \quad m = \text{A, B} \quad k = \text{r, s, t} \tag{4}$$

where $V_{mmc\_mkj}^{*}$ is the output DC voltage command of each cell. i is the index of the cell number. Moreover, m shows an index which is the upper side A or the lower side B. k is an index of each phase. m, k and j are matched in both side of (4). A_{vd_mkj} is a dividing ratio of each cell which is varied depending on the capacitor voltage.

The dividing ratio which is generated by the proposed control system is given by (5).

$$A_{vd\_mkj} = \frac{1}{2} \frac{v_{cmkj}}{\sum_{x=1}^{n/2} v_{cmkx}} \quad m = \text{A, B} \quad k = \text{r, s, t} \tag{5}$$

where V_{cmkj} is each capacitor voltage. The denominator of (5) is the summation of all capacitor voltages in each arm. The dividing ratio A_{vd_mkj} is set into $1/n$ when the all capacitor voltages in the arm are same. On the other hand, the dividing ratio A_{vd_mkj} is varied depending on the capacitor voltage when each capacitor voltage fluctuates.

For example, the dividing ratio A_{vd_mkj} of the cell is set into high when its capacitor voltage is higher than the command of the capacitor voltage. Thus, the output power of that cell becomes high because the output DC voltage of the cell is high due to the high dividing ratio. Therefore, the electric charge of the capacitor is discharged. In contrast, the dividing ratio A_{vd_mkj} of the cell is set into low when its capacitor voltage is lower than the command. Thus, the electric charge of the capacitor is charged because the output power of the cell becomes low due to the low dividing ratio. The main advantage of the proposed voltage balancing control system is that it is not necessary to design control parameters because the dividing ratio A_{vd_mkj} is adjusted automatically depending on the capacitor voltage. Thus, the proposed voltage balancing control system is simpler than the conventional control system.

IV. Clarification of Total Electrostatic Energy in Cell Capacitors

Each cell of the MMC has the capacitor. However, the volume of the capacitors has not been discussed thoroughly. As one of reasons, the capacitor which is considered to apply to the cell has the special specification such as the high voltage rating and the high capacitance. The above capacitor has a low number of product data due to these special specifications. On the other hand, as the common view of the capacitor volume, the volume of the capacitor becomes large when the voltage rating is high and the capacitance is large. Hence, the volume of the capacitors varies based on the electrostatic energy which is the function of the voltage rating and the capacitance. Thus, the evaluation method of the capacitor volume has been reported in terms of the electrostatic energy of the capacitors [8]. However, in the above evaluation, types of the capacitors have not been discussed.

In general, an electrolytic capacitor is known as the capacitor which has the high capacity. The ripple current of the capacitor is one of the important factors for the design of the MMC when the electrolytic capacitors are applied to the MMC, because the ripple current affects the lifetime of the capacitors. Moreover, the voltage rating of the capacitor drastically changes according to the number of cells, whereas the ripple current also changes depending on the voltage rating and the capacitance.

In this paper, the ripple current is applied as one of evaluation indexes in order to evaluate the volume of the capacitors. Additionally, the relationship between the capacitor volume and the ripple current is evaluated from a database of commonly-marketed electrolytic capacitors which are generally implemented into products.

A. Calculation of capacitor's voltage rating

The output DC voltage's command in the MMC V_{mmc}^{*} is added to the output block of the input current control. In the MMC, the output DC voltage V_{mmc} is applied in each leg because each leg is connected to the load in parallel. In addition, the maximum value of the input phase voltage is applied to each arm. Therefore, each capacitor voltage depends on both the input voltage and output voltage. The capacitor voltage command v_c^{*} is given by (6). Note that the modulation index λ is set to 0.8 or less. Besides, the voltage drop of the buffer inductor is ignored because the voltage drop of the buffer inductor is sufficiently small compared with the input phase voltage and the output voltage of the MMC.

$$v_c^* \geq \frac{1}{n\lambda}\left(2\sqrt{\frac{2}{3}}E + V_{mmc}^*\right) \tag{6}$$

B. Calculation of ripple voltage

In general, the capacitance of the converter is designed based on the ripple voltage against the average value of the capacitor voltage. Additionally, it is important to clarify the formula of the capacitor voltage in order to design the fluctuation of the capacitor voltage. On the other hand, in the MMC, the system has many capacitors and the voltage rating of the capacitor changes depending on the number of cells. Furthermore, the formula of the capacitor voltage which includes the circuit parameters of the MMC should be clarified.

First, the cell output voltage v_{cell} is given by (7) in order to control the input current and the output DC voltage. The arm current i_{arm} is given by (8). The arm current i_{arm} includes the AC component and the DC component. The AC current flows from the generator in order to maintain the capacitor voltage. On the other hand, the DC current flows into the load in order to supply the power. Moreover, the arm current i_{arm} flows into each cell in same arm. Note that the sign of positive or negative is decided based on the lower arm of Fig. 1.

$$v_{cell}(t) = \frac{1}{n}\left(2\sqrt{\frac{2}{3}}E\sin\omega t + V_{mmc}\right) \tag{7}$$

$$i_{arm}(t) = -\frac{1}{2}\sqrt{\frac{2}{3}}\frac{S}{E}\sin(\omega t - \phi) + \frac{P}{3V_{mmc}} \tag{8}$$

where S is an input apparent power. P is an input active power. Q is an input reactive power. ϕ is an input phase difference. Moreover, S is defined by (9).

$$S = \sqrt{P^2 + Q^2} \tag{9}$$

From (7) and (8), the instantaneous power of the cell is calculated. The energy which flows into the capacitor is calculated by integration of the instantaneous power. The energy which flows into the capacitor is given by (10).

$$\begin{aligned} W_C(t) &= \int v_{cell} i_{arm} dt \\ &= \frac{1}{2}\sqrt{\frac{2}{3}}\frac{V_{mmc}S}{n\omega E}\cos(\omega t - \phi) - \frac{2}{3}\sqrt{\frac{2}{3}}\frac{EP}{n\omega V_{mmc}}\cos\omega t \\ &\quad + \frac{S}{6n\omega}\sin(2\omega t - \phi) + W_{C0} \end{aligned} \tag{10}$$

where W_{C0} is the constant of integration.

W_{C0} does not change with time. Thus, W_{C0} is defined as the average value of the energy which flows into the capacitor. Moreover, the relationship between the capacitor voltage $v_c(t)$ and the energy which flows into the capacitor $W_C(t)$ is given by (11) in terms of an electrostatic energy.

$$W_C(t) = \frac{1}{2}Cv_C(t)^2 \tag{11}$$

From (10) and (11), the capacitor voltage $v_c(t)$ is given by (12). Note that the theoretical formula is calculated in the linear approximation by Taylor expansion.

$$\begin{aligned} v_c(t) &= V_{C0} + \frac{1}{2}\sqrt{\frac{2}{3}}\frac{V_{mmc}S}{n\omega CEV_{C0}}\cos(\omega t - \phi) \\ &\quad - \frac{2}{3}\sqrt{\frac{2}{3}}\frac{EP}{n\omega CV_{mmc}V_{C0}}\cos\omega t \\ &\quad + \frac{S}{6n\omega CV_{C0}}\sin(2\omega t - \phi) \end{aligned} \tag{12}$$

where the constant value ${V_{C0}}^2$ is defined by $2W_{C0}/C$.

The ripple voltage includes the fundamental frequency component whose frequency is same as the generator voltage's frequency and the high frequency component whose frequency is as twice as the frequency component of the generator voltage's frequency (second-order frequency component). Moreover, V_{C0} is defined as the average value of the capacitor voltage because W_{C0} does not change with time.

C. Analysis of ripple voltage

From (12), it is understood that the ripple voltage with the fundamental frequency is function of the input phase difference ϕ because the input active power P changes depending on the input phase difference ϕ. Therefore, the relationship between the input phase difference ϕ and the ripple voltage has to be clarified in order to design the capacitance for the worst case when a magnitude of the ripple voltage is the largest. The ripple voltage with the fundamental frequency $\Delta v_{c\_1}(t)$ is given by (13). Note that (13) is calculated by synthesizing fundamental frequency components of (12). An angle β is given by (14).

$$\begin{aligned} &\Delta v_{c\_1}(t) = \\ &-\sqrt{\frac{2}{3}}\frac{S}{n\omega CV_{C0}}\left\{\left(\frac{E}{3V_{mmc}}\right)^2 + \left(\frac{E}{3V_{mmc}} - \frac{V_{mmc}}{2E}\right)^2\right. \\ &\left. + 2\left(\frac{E}{3V_{mmc}}\right)\left(\frac{E}{3V_{mmc}} - \frac{V_{mmc}}{2E}\right)\cos 2\phi\right\}^{\frac{1}{2}} \cos(\omega t + \phi + \beta) \end{aligned} \tag{13}$$

$$\beta = \tan^{-1}\left[\frac{-\left(\frac{E}{3V_{mmc}} - \frac{V_{mmc}}{2E}\right)\sin 2\phi}{\left(\frac{E}{3V_{mmc}}\right) + \left(\frac{E}{3V_{mmc}} - \frac{V_{mmc}}{2E}\right)\cos 2\phi}\right] \tag{14}$$

From (13), it is understood that the magnitude of the ripple voltage with the fundamental frequency becomes maximum when the input phase difference ϕ is 0 or π.

Fig. 4 shows the relationship between the input phase difference ϕ and the ripple voltage. In Fig. 4, the fundamental frequency component is drawn by (13). The second-order frequency component is drawn by the last term of (12). As a result, the second-order frequency component of the ripple voltage does not changed against the input phase difference because the input apparent power S does not change. On the other hand, the

fundamental frequency component becomes maximum when the input phase difference ϕ is 0 or π. Thus, it is necessary to design the capacitance only when the input phase difference ϕ is 0.

D. Clarification of total static energy

In general, the ripple voltage is evaluated as the ripple factor. Moreover, the ripple factor is defined by (15) [10].

$$A_{ripple} = \frac{\Delta v_{C\_peak\text{-}to\text{-}peak}}{2V_{C0}} \tag{15}$$

where A_{ripple} is the ripple factor and $\Delta v_{c\_peak\text{-}to\text{-}peak}$ is the fluctuation range of the ripple voltage. Note that the fluctuation range equals to the peak-to-peak value of the ripple voltage when amplitude of the ripple voltage is symmetric about the average voltage.

In addition, from the previous section, it is necessary to design the capacitance when the input phase difference ϕ is 0. Thus, the ripple factor is defined when the input phase difference ϕ is 0. From (13) and (15), the ripple factor of the fundamental frequency component is given by (16). Note that ϕ in (13) is 0 and S is replaced by P because Q is zero.

$$A_{ripple} = \sqrt{\frac{2}{3}} \frac{P}{n\omega C V_{C0}^{\ 2}} \left(\frac{2}{3}\frac{E}{V_{mmc}} - \frac{1}{2}\frac{V_{mmc}}{E} \right) \tag{16}$$

Moreover, from (6) and (16), the capacitance C is calculated by (17). Note that the capacitor voltage V_{C0} equals to the command of the capacitor voltage.

$$C = \sqrt{\frac{2}{3}} \frac{n\lambda^2 P}{\omega A_{ripple}} \frac{1}{\left(2\sqrt{\frac{2}{3}}E + V_{mmc} \right)^2} \left(\frac{2}{3}\frac{E}{V_{mmc}} - \frac{1}{2}\frac{V_{mmc}}{E} \right) \tag{17}$$

The required capacitance C to suppress the ripple voltage according to the ripple factor A_{ripple} is calculated by (17). Moreover, the required capacitance becomes large with increasing the number of cells n when the ripple factor A_{ripple} is not changed at any number of cells. It means that the ripple voltage becomes large relatively because the average value of the capacitor voltage becomes small with increasing the number of cells.

Finally, the total electrostatic energy E_{C_sum} is clarified. The electrostatic energy is calculated by replacing the parameters in function (11) by (6) and (17). Additionally, it is able to calculate the total electrostatic energy to multiple total numbers of cells $3n$. Thus, the total electrostatic energy is given by (18).

$$\begin{aligned} E_{C\_sum} &= \frac{3n}{2} C V_{C0}^{\ 2} \\ &= \frac{3}{2}\sqrt{\frac{2}{3}} \frac{P}{\omega A_{ripple}} \left(\frac{2}{3}\frac{E}{V_{mmc}} - \frac{1}{2}\frac{V_{mmc}}{E} \right) \end{aligned} \tag{18}$$

The formula (18) implies that the total electrostatic energy does not change when the ripple factor A_{ripple} is constant at any number of cells. Thus, it is difficult to evaluate the relationship between the total volume of the capacitors and the number of cells in terms of the total electrostatic energy when the ripple factor is constant.

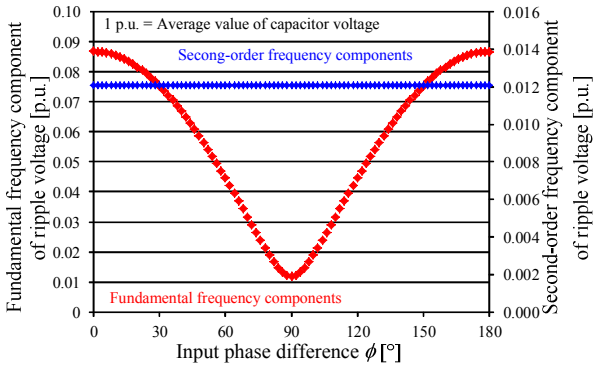

Fig. 4. Relationship between the input phase difference ϕ and the ripple voltage. The fundamental frequency component is calculated by (13) and the second-order frequency component is calculated by the last term of (12). The magnitude of the fundamental frequency components is the maximum when the input phase difference ϕ is 0 or π.

E. Clarification of ripple current

In general, the ripple current value of the capacitor is shown in the datasheet of commonly-marketed electrolytic capacitors which are generally implemented into products. Moreover, the capacitor should be selected in order that the ripple current value which flows to each capacitor is sufficiently small compared with the specified value on each datasheet in terms of the lifetime. Additionally, the number of the capacitors which are connected in parallel on each cell should increase in order to meet the specified value of the ripple current. Therefore, this makes the capacitor volume change drastically. Thus, the relationship between the ripple current and the capacitor volume has to be clarified before the relationship between the number of cells and the capacitor volume is evaluated.

The relationship between the capacitor current i_c and the capacitor voltage v_c is given by (19).

$$i_C = C\frac{dv_C}{dt} \tag{19}$$

From (13) and (19), it is concluded that the relationship between the input phase difference ϕ and the maximum value of the amplitude does not change after the differential of the ripple voltage. Therefore, the amplitude is maximum when ϕ is 0. Thus, the maximum effective value of the ripple current I_{C_1} is given by (20).

$$I_{C\_1} = \sqrt{\frac{1}{3}} \frac{\lambda P}{\left(2\sqrt{\frac{2}{3}}E + V_{mmc} \right)} \left(\frac{2}{3}\frac{E}{V_{mmc}} - \frac{1}{2}\frac{V_{mmc}}{E} \right) \tag{20}$$

From (20), it is understood that the maximum effective value of the ripple current does not change when the number of cells and the capacitance changes.

V. Experimental Result

In this section, experimental results by the miniature model of the step-down rectifier using the MMC are shown. In the experiment, a utility power source of 200 V is applied as the input voltage source.

Fig. 5 shows waveforms of the input phase voltage, the input current and the output DC voltage. Firstly, from the waveforms of the input phase voltage and the input current, it is confirmed that the unity power factor is obtained in the input side. Moreover, the total harmonic distortion (THD) of the input current is 5.6%. Second, the waveform of the output DC voltage in lower side of Fig. 5 shows that the miniature model converts from the input voltage of 200 V into the output DC voltage of 65 V. From this result, it is confirmed that the output voltage is kept constant. Therefore, the miniature model of the MMC achieves the step-down rectification.

Fig. 6 shows the waveforms of cell capacitor voltages which are connected to the r-phase leg. The cell capacitor voltage is controlled according to the capacitor voltage command. As a result, the proposed system maintains the capacitor voltage of each H-bridge cell to the voltage command of 120 V. In addition, the maximum voltage error between the voltage command of the cell capacitor and the measured voltage is 5% or less.

VI. Evaluation of Capacitor Volume

The overall volume of the capacitors is evaluated by using the database of commonly-marketed electrolytic capacitors which are generally implemented into many products. Conditions to make the database are as follows;

a) Evaluated targets are the capacitors which each manufacturer (Nippon Chemi-Con, Nichicon and Rubycon) recommends as “For inverters” and “For high power application”.

b) Withstand voltages are from 100 V to 600 V.

c) Each capacitor volume is the average value in the capacitor volumes of each ripple current value which is rounded the ripple current of the capacitor to unit.

A. Relationship between ripple current and capacitor volume

Fig. 7 shows the relationship between the ripple current and the capacitor volume as a database example. The figure in the graph shows the ripple current of one capacitor. Therefore, the number of the capacitors which are connected in parallel on one cell increases with increasing the ripple current. Moreover, the start point of each line means the ripple current and the volume of one capacitor. As a result, the overall volume of the capacitors becomes small by connecting the capacitor with the small ripple current in parallel, compared with using one capacitor with the large ripple current. Thus, the parallel connection of the capacitor with the small ripple current is better than using one capacitor with the large ripple current in order to achieve the size reduction of capacitors. Moreover, the ripple current does not change against the capacitance and the number of cells. Thus, the minimum point of capacitor volume against the number of cells achieves the minimum point of the overall volume.

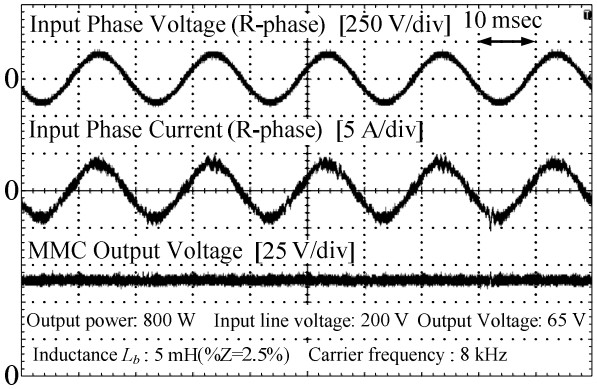

Fig. 5. Waveforms of input voltage, input current and output voltage. The unity power factor is obtained in the input stage. The THD of the input current is 5.6% when the %Z of the inductor is 2.5%.

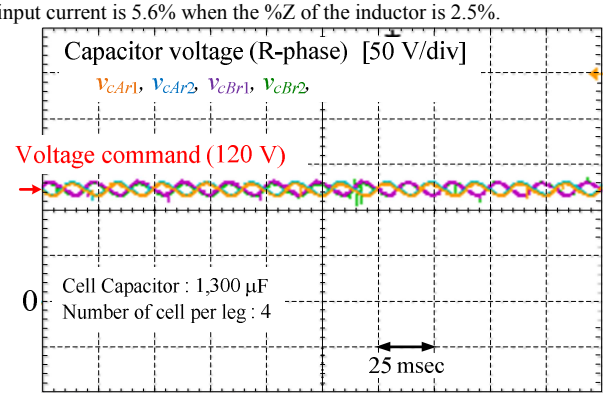

Fig. 6. Waveforms of the capacitor voltage in r-phase leg. The proposed system maintains the capacitor voltage of each H-bridge cell to the voltage command of 120 V. In addition, the maximum error between the capacitor voltage command and the measured voltage is 5% or less.

B. Relationship between number of cells and capacitor volume

Fig. 8 shows the relationship between the number of cells and the capacitor volume. Note that the number of series connection capacitors increases when the charge voltage which is calculated by (6) is larger than the withstand voltage. Additionally, the charge voltage is set 30% more than the value which is calculated by (6). In this evaluation, the capacitor volume is determined by the multiplied value of the number of series connection capacitors and the number of cells. The capacitor volume changes drastically when the number of cells is small, because both factors changes. On the other hand, the capacitor volume increases linearly as the number of cells increases when the number of series connection capacitors is kept constant. Moreover, there are several points which the capacitor volume is minimum.

Fig. 9 shows the ratio of the charge voltage to the withstand voltage. The ratio is defined as a voltage utilization factor. Fig. 9 shows that the number of cells which the capacitor volume becomes minimum, and the number of cells which the voltage utilization factor closest to 1.0 match. On other words, it is possible to achieve the volume minimization by closing the voltage utilization factor to 1.0. As a conclusion, it is necessary to meet following conditions in order to achieve the volume minimization of the capacitors.

1) Applying the capacitor with the small ripple current

2) Maximizing the voltage utilization factor

VII. CONCLUSION

This paper discussed the overall volume evaluation of capacitors by applying a database of commonly-marketed electrolytic capacitors which are generally implemented into many products. Specifically, the relationship between the capacitor volume and the number of cells are considered. It is necessary to consider the ripple current in terms of the lifetime when the electrolytic capacitor is applied to the MMC. Thus, the number of capacitors changes drastically due to the ripple current of one capacitor. In this paper, the number of parallel connection capacitors is evaluated in terms of the ripple current. Moreover, the number of series connection capacitors is evaluated in the terms of the voltage utilization factor. As a conclusion, it is necessary to meet following conditions in order to achieve the volume minimization of capacitors.

1) Applying the capacitor with the small ripple current
2) Maximizing the voltage utilization factor

As a future work, the design method including the thermal design by the loss analysis in order to achieve the volume minimization of the MMC will be considered.

REFERENCES

[1] H. Kakigano, Y. Miura, and T. Ise, "Low-Voltage Bipolar-Type DC Microgrid for Super High Quality Distribution," IEEE Trans. on Power Electronics, Vol.25, No.12, pp.3066-3075 (2010)

[2] D. Salomonsson, L. Söder, and A. Sannino, "Protection of Low-Voltage DC Microgrids," IEEE Trans. on Power Delivery, Vol.24, No.3, pp.1045-1053 (2010)

[3] T. Senju, T. Nakaji, K. Uezato, and T. Funabashi, "A Hybrid Power System Using Alternative Energy Facilities in Isolated Island," IEEE Trans. on Energy conversion, Vol.20, No.2, pp.406-414 (2005)

[4] F. Blaabjerg, R. Teodorescu, M. Liserre, and A. V. Timbus, "Overview of Control and Grid Synchronization for Distributed Power Generation Systems", IEEE Trans. on Industrial Electronics, Vol.53, No.5, pp.1398-1408 (2006)

[5] K. Inomata, H. Hara, H. Morimoto, S. Fujii, J. Takeda, E. Yamamoto, E, Watanabe, and J. Kang, "Enhanced Fault Ride Through Capability of Matrix Converter for Wind Power System," IECON2013, pp.4838-4843 (2013)

[6] T. Nakanishi, J. Itoh: "Modular Multilevel Converter for Wind Power Generation System connected to Micro-grid" ICRERA2014, No.219, (2014)

[7] N. Thitichaiworakorn, M. Hagiwara, and H. Akagi, "Experimental Verification of a Modular Multilevel Cascade Inverter Based on Double-Star Bridge Cells," IEEE Trans. on Industry applications, Vol.50, No.1, pp.509-519 (2014)

[8] S. P. Engel. R. W. De Doncker, "Control of the Modular Multi-Level Converter for minimized cell capacitance," EPE2011 (2011)

[9] K. Wang, Y. Li, Z. Zheng, and L. Xu, "Voltage Balancing and Fluctuation-Suppression Methods of Floating Capacitors in a New Modular Multilevel Converter," IEEE Trans. on Industry electronics, Vol.60, No.5, pp.1943-1954 (2013)

[10] Y. Ohnuma, and J. Itoh, "A Single-phase Current Source PV Inverter with Power Decoupling Capability using an Active Buffer," IEEE Trans. on Industry applications, Vol.51, No.1, pp.531-538 (2014)

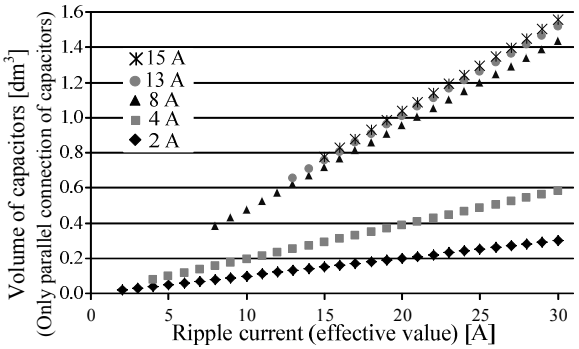

(a) Withstand voltage : 100 V, Endurance : 85℃, 5000hour

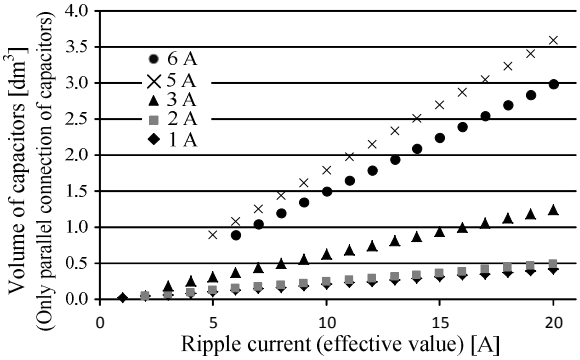

(a) Withstand voltage : 400 V, Endurance : 105℃, 3000hour

Fig. 7. Relationship between the ripple current and the capacitor volume. The parallel connection of the capacitor with the small ripple current is better than using one capacitor with the large ripple current in order to achieve the size reduction of capacitors.

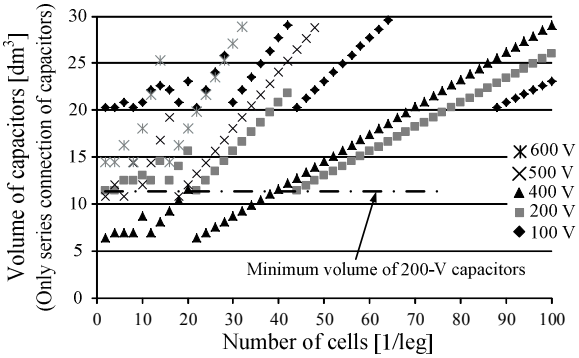

Fig. 8. Relationship between the number of cells and the capacitor volume. The capacitor volume is determined by the multiplied value of the number of series connection capacitors and the number of cells. The capacitor volume changes drastically when the number of cells is small, because both the number of series connection capacitors and the number of cells changes. On the other hand, the capacitor volume increases linearly with increasing the number of cells when the number of series connection capacitors is kept constant.

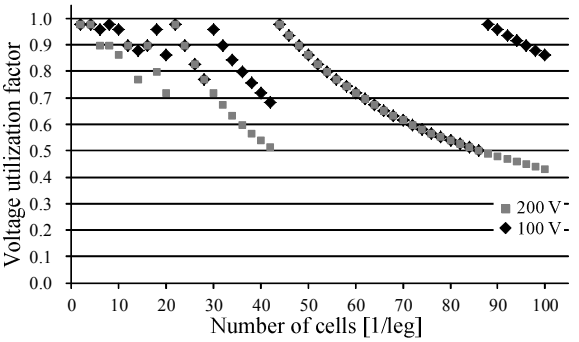

Fig. 9. Relationship between a voltage utilization factor and the number of cells. The number of cells which the capacitor volume becomes minimum, and the number of cells which the voltage utilization factor closest to 1.0 match.